NASA Technical Memorandum 105393
AIAA–92–0274

Analysis of an Advanced Ducted Propeller Subsonic Inlet

Chanthy Iek and Donald R. Boldman
Lewis Research Center
Cleveland, Ohio

and

Mounir Ibrahim
Cleveland State University
Cleveland, Ohio

Prepared for the
30th Aerospace Sciences Meeting and Exhibit
sponsored by the American Institute of Aeronautics and Astronautics
Reno, Nevada, January 6–9, 1992

NASA

Analysis of an Advanced Ducted Propeller Subsonic Inlet

Chanthy Iek*, Donald R. Boldman**
National Aeronautics and Space Administration
Lewis Research Center
Cleveland, Ohio 44135

Mounir Ibrahim***
Cleveland State University
Cleveland, Ohio 44115

Abstract

A time marching Navier-Stokes code called PARC (PARC2D for 2-D/axisymmetric and PARC3D for 3-D flow simulations) was validated for an advanced ducted propeller (ADP) subsonic inlet. The code validation was implemented for a non-separated flow condition associated with the inlet operating at angles-of-attack of 0° and 25°. The inlet test data were obtained in the 9 x 15 ft Low Speed Wind Tunnel at NASA Lewis Research Center as part of a cooperative study with Pratt and Whitney. The experimental study focused on the ADP inlet performance for take-off and approach conditions. The inlet was tested at a free stream Mach number of 0.2, at angles-of-attack between 0° and 35°, and at a maximum propeller speed of 12,000 RPM which induced a corrected air flow rate of about 46 lb/sec based on standard day conditions. The computational grid and flow boundary conditions (BC) were based on the actual inlet geometry and the tunnel flow conditions. At the propeller face, two types of BC's were applied; namely, a mass flow BC and a fixed flow properties BC. The fixed flow properties BC was based on a combination of data obtained from the experiment and calculations using a potential flow code. Comparison of the computational results with the test data indicates that the PARC code with the propeller face fixed flow properties BC provided a better prediction of the inlet surface static pressures than the prediction when the mass flow BC was used. For an angle-of-attack of 0°, the PARC2D code with the propeller face mass flow BC provided a good prediction of inlet static pressures except in the region of high pressure gradient. With the propeller face fixed flow properties BC, the PARC2D code provided a good prediction of the inlet static pressures. For an angle-of-attack of 25° with the mass flow BC, the PARC3D code predicted static pressures which deviated significantly from the test data; however, with the fixed flow properties BC, a good comparison with the test data was obtained.

Nomenclature

D	diameter
h	distance from the wall
L	shroud length
l	axial distance from propeller face to rake total pressure probes
M	Mach number
p	static pressure

*Aerospace Research Engineer

**Aerospace Research Engineer
Assoc. Fellow AIAA

***Assoc. Professor
Member of AIAA

P	total pressure
W	mass flow rate
X	axial distance from propeller face
α	angle-of-attack
ϕ	circumferential angle

Subscripts

c	corrected to standard day conditions
loc	local condition
prop	propeller face
0	free stream conditions

Introduction

Flow characteristics associated with a subsonic ducted propeller inlet vary from a simple axisymmetric to a complex 3-D flow with primary and secondary flow interaction as the angle-of-attack (α) increases. In addition, the presence of an operating propeller produces blockage and suction effects on the flow. The propeller rotation also induces a flow swirl motion at the propeller face. Since the flow is subsonic these effects generated by the propeller can influence the upstream flow conditions.

An analytical study done by D. Boldman et. al.[1] used a panel code in predicting the performance of three different designs of advanced ducted propeller (ADP) inlets operating at take-off and approach conditions. For a non-separated inlet flow, the predicted results of surface pressures were in good agreement with the test data. The code incorporated a compressibility correction of Lieblein and Stockman[2], but its fundamental approach is based on the potential flow method. In a subsonic inlet application, a variety of flow behaviors occur due to wall and turbulent viscous effects, formed shock waves, and separation all of which are attributed to the nature of the viscous, compressible, rotational flow characteristics. This type of complex flow phenomena cannot be predicted by a panel code, thus requiring a Navier-Stokes based code for an analysis.

The objective of the present study was to validate a Navier-Stokes based CFD code for the prediction of these complex subsonic inlet flows. Although the current calculations were limited to unseparated flow, this effort represents a first step in the validation process leading to the prediction of more complicated flows with separation. Validation of this code was based on experimental data from an ADP inlet which was tested in the 9 x 15 ft Low Speed Wind Tunnel at NASA Lewis Research Center (LeRC). The experimental program was performed as a cooperative study with Pratt and Whitney.

The PARC code (PARC2D for 2D/axisymmetric and PARC3D for 3D flow simulations) was selected for the subsonic inlet flow computations. The PARC3D code was originally developed by Pulliam and Steger[3] as AIR3D. Pulliam[4] later added the Jameson[5] artificial dissipation and changed the name to ARC3D. Cooper[6] modified the code for internal flow in propulsion applications and named the code PARC3D. The PARC code either for 2-D or 3-D flow simulation is a time marching Reynolds averaged Navier-Stokes solver which utilizes the Beam and Warming approximate factorization. The code uses a central differencing numerical scheme on a generalized curvilinear coordinate system with implicit second order and explicit fourth order artificial dissipations. The turbulent model used in the PARC code is the Baldwin-Lomax model. An important feature of the PARC code is its capability to compute flows about complex geometries. Physical and computational boundaries may be located on any portion of the grid. Also, the PARC code allows a complex geometry to be sub-divided into a multiple-block grid with each block having multiple computational BC's. The code incorporates the semi-automatic time-step control function which allows a flow simulation to start from a nearly arbitrary initial condition.

In the present paper, subsonic inlet flow computations were performed at angles-of-attack of 0° and 25° by PARC2D and PARC3D respectively. Two different boundary conditions were used in the code for the propeller face. These boundary conditions (mass flow and fixed flow properties) were studied with both PARC2D and PARC3D codes. Analytical results are compared with experimental results.

Experimental Configuration

The typical ADP simulator was installed in the wind tunnel as shown in figure 1. The simulator was rotated about the pivot axis in a counterclockwise direction to set the inlet angle-of-attack position. The maximum α attainable was 35°. The propeller was driven by a 1,000 HP air turbine drive system at rotational speeds up to 12,000 RPM.

One of the inlet designs studied in the experimental program and selected for this code validation study is

shown in figure 2(a). The axisymmetric inlet configuration consists of a cowl and a center body. The center body rotates with the propeller. Inlet data obtained for comparison with the computational results included cowl axial static pressures and boundary layer total pressure distributions. The cowl axial static pressure taps were located at ϕ = 0° and ϕ = 180°. Figure 2(b) shows the locations of the boundary layer total pressure rakes and pressure recovery rakes. Both sets of total pressure rakes were normally installed together during testing. However, in some tests all of the rakes were removed from the inlet to check the effect of these rakes on the inlet performance.

The test data were taken for a nominal free stream Mach number (M_0) of 0.2, α's from 0° to 35°, and at propeller speeds from 7,500 to 12,000 RPM. The average total pressure rise across the propeller was 1.25 times the free stream total pressure at a propeller speed of 12,000 RPM. The corrected air flow rates (W_c) ranged from 31 to 46 lb/sec. Two sets of test data from this extensive data base were selected for comparison with the computational results. These two sets of data included α's of 0° and 25°, at a W_c of 46 lb/sec and M_0 of 0.2.

Computations

Computations were performed on the Cray-YMP computer at the NASA LeRC. The computational grids for the axisymmetric (α = 0°) and for 3-D (α = 25°) flow calculations are shown in figures 3 and 4, respectively. Two types of grids were evaluated, the H-grid and the H-grid with an embedded C-grid (HC-grid). Figure 3 shows a total of six blocks forming the H-grid and a total of seven blocks forming the HC-grid. The additional block in the HC-grid is the embedded C-grid in the computational domain H-grid. Figure 3 also shows the grid size for each block in terms of a matrix with the first and second digits representing the numbers of grid points along the axial and transverse directions, respectively. The computational 3-D grid (fig. 4) was developed by rotating the 2-D grid (fig. 3) in 50 increments circumferentially through 180°. These grid blocks were designed to perform simultaneously a combination of viscous and inviscid flow calculations. A viscous calculation was performed on the first three blocks of the H-grid and on the first four blocks of the HC-grid including the C-grid. An inviscid computation was performed on the other three blocks for both the H-grid and the HC-grid. The reason for this inviscid calculation was to generate a flow solution that closely simulated the actual flow conditions aft of the inlet nacelle with the exception of a possible swirl motion produced by the propeller. During the code execution, the results generated by this inviscid calculation were fed across the block-interface boundary at the nacelle trailing edge for the viscous calculation and vice versa. Thus, the flow solution at this boundary served as a computational BC, rather than a one-time-prescribed BC. This BC evolved through iterative calculations with the final solution consisting of the results shared by the adjoining blocks on both sides.

Computational boundary conditions consisted of total and static pressures, total and static temperatures, and an inlet angle-of-attack of 0° or 25°. Viscous and inviscid calculations were implemented by specifying the wall surface BC's as no-slip and slip conditions and simultaneously executing the PARC code in fully viscous turbulent and inviscid modes. Two types of BC's were applied at the propeller face; namely mass flow BC (mass BC) and a fixed flow properties BC (fixed BC). The mass BC was prescribed as the inlet actual mass flow. The PARC code computed the static pressures and temperatures through iterative calculations until they reached conditions that satisfied the prescribed value of this mass flow. This was an indirect means of prescribing the static pressure and static temperature BC, termed a free BC. In this case, the mass BC is preferred over the free BC because the static values of pressure and temperature are not known a priori, especially for the 3-D flow. With the propeller face mass BC, only the HC-grid was used in the PARC flow computations for both values of angle-of-attack. The propeller fixed BC was developed by using data obtained from a combination of experiment and calculations by the HESS panel method[7] as shown in figures 5 and 6. The experimental data were the measured circumferential static pressures on the cowl at a station located at 0.46 inches upstream of the propeller face. During testing, the center body rotated with the propeller making it impractical to measure the static pressure on the center body. In order to circumvent this problem, the HESS code was selected to compute the potential flow for the inlet at the desired values of M_0, α, and W_c. The HESS code yielded a profile of circumferential static pressures on the center body 0.46 inches upstream of the propeller face. This calculated static pressure profile was coupled with the cowl measured static pressure profile and iterated based on the measured W_c to obtain a new static pressure profile called an adjusted profile as shown in figures 5 and 6. This new adjusted static pressure profile on the

center body and the experimental static pressure profile on the cowl were interpolated linearly in the radial direction to obtain flow properties and velocity distributions for every grid point of the propeller face grid section. These interpolated distributions were maintained as the propeller face fixed BC's for the PARC code computation. With the propeller face fixed BC, both the H-grid and the HC-grid were used in the PARC flow computations.

The operation of the propeller produced an average total pressure rise of about 1.25 times the free stream total pressure for both α's of 0° and 25°. In the computation, a BC specification was made in terms of total pressure and total temperature at the propeller exit plane to account for this increase in total pressure. At the nozzle core exit (fig. 3), the BC was specified for flow leaving the system with its total pressure and total temperature equal to the free stream values.

Results and Discussion

In the experimental study, the ADP inlet was tested with and without the boundary layer and total pressure recovery rakes (fig. 2). The computational grids for the axisymmetric and the 3-D flow calculations did not include any of these rakes, so the computational results represent flow through the inlet without rakes. A comparison of experimental and predicted boundary layer total pressures was made. Since the presence of the rakes had an influence on the measured static pressures, the computational results were compared with the test data obtained for both cases. The computations did not incorporate flow swirl which could be induced by the rotation of the propeller and the center body. The PARC code permits incorporation of a flow swirl BC, but it was not applied since there was insufficient information to determine the level of swirl and its interaction with the inlet flow. The static and total pressure ratios presented herein are ratios of local static and local total pressures to the free stream total pressure. In this study, it took a total of about 2 hours of Cray-YMP CPU time for a PARC2D axisymmetric flow computation and a total of about 80 hours for a PARC3D flow computation.

The Mach number contours presented in figure 7 are PARC2D computational results for an inlet flow condition at α = 0°, M_0 = 0.2, and W_c = 46.4 lb/sec based on standard day conditions. Figure 7(a) shows Mach number contours of inlet nacelle internal and external flows. Figure 7(b) shows Mach number contours resulting from computation using the mass BC at the propeller face. Figure 7(c) shows two distributions of Mach number contours obtained from computations using the fixed BC at the propeller face and with the HC-grid and the H-grid, respectively. With the HC-grid and mass BC, the Mach number contours display flow characteristics which are similar to those obtained with the fixed BC (fig. 7(c)). Similar distributions were also observed for Mach number contours resulting from the H-grid and the HC-grid.

A comparison of the inlet cowl axial static pressure ratios for the experiment and analysis is shown in figure 8. The experimental results include data from inlet tests with and without the boundary layer and total pressure recovery rakes (fig. 2). The installation of these total pressure rakes had an effect on internal flow from the propeller plane (X = 0) to near the inlet highlight. Computational static pressure ratio distributions include results obtained from the mass BC and the fixed BC at the propeller face. With the fixed BC there are two distributions resulting from the use of the H-grid and the HC-grid. The comparison shows that the mass BC distribution deviates from the test data (without rakes) in the region of low static pressure. Based on this mass BC, the calculated value of static pressure ratio at the propeller face was p_{loc}/P_0 = 0.851. By referring to figure 5 it can be noted that this pressure ratio is slightly higher than the average cowl circumferential static pressure ratio near the propeller face. This difference could be a reason for the deviation in the comparison shown in figure 8. The other two distributions resulting from the fixed mass BC compare more favorably with the test data from the inlet without rakes. This latter result was expected since the computational grids did not include these rakes. The comparison shows that the difference in the grid format for the fixed BC did not have any significant impact on the solutions.

A comparison of experimental and predicted total pressure ratios is shown in figure 9. The experimental total pressures were measured by a boundary layer rake located 3.0 inches (0.17 D_{prop}) upstream of the propeller face and at a circumferential position of ϕ = 160°. The calculated total pressure distributions using the HC-grid compare well with the test data, and the different types of BC's did not affect the boundary layer flow solution at this location. The distribution resulting from using the H-grid with the fixed BC at the propeller face was significantly different from the test data. This difference could be attributed to the fact that the grid resolution at this location was more closely packed for the embedded

C-grid than for the H-grid. The value of Y^+ at the first grid point from the surface was 5 for the C-grid and 15 for the H-grid. However, this assessment is not definitive and more analysis needs to be done.

Figure 10 shows Mach number contours resulting from the PARC3D computation for M_0= 0.2, α = 25°, and W_c = 46.6 lb/sec based on standard day conditions. The Mach number contours in figure 10(a) characterize the 3-D inlet nacelle internal and external flows. Figures 10(b) and 10(c) show Mach number contours resulting from using the mass BC and the fixed BC, respectively at the propeller face. With the HC-grid, the mass BC Mach number contours in figure 10(b) are more uniform over the windward (ϕ = 0°) and leeward (ϕ = 180°) sides than for the fixed BC Mach number contours (fig. 10(c)). With the fixed BC, the two grids (HC and H) display similar patterns of Mach number contour lines as shown in figure 10(c). The Mach number contours are shown only over the inlet plane of symmetry to emphasize different flow characteristics on the windward (ϕ = 0°) and on the leeward (ϕ = 180°) sides.

Figures 11 and 12 show a comparison of experimental static pressure ratios with those resulting from PARC3D computations using the mass BC and the fixed BC at the propeller face, respectively. The experimental data in figure 11 include two distributions of static pressure ratios resulting from the inlet tested with and without the total pressure rakes (fig. 2). As in the case of α = 0° (fig. 8), the installation of the rakes in the inlet induced an effect on the flow upstream, especially around the region of low static pressure. One reason could be that the rakes produced a certain amount of blockage in the flow passage, and since the flow is subsonic, this blockage is sensed by the flow upstream resulting in an increase in the local static pressure. In figure 11(a), the calculated static pressure ratio distribution on the windward side (ϕ = 0°) compares favorably with the test data. However, on the leeward side (ϕ = 180°) shown in figure 11(b), the calculated distribution dropped below the test data over the inside surface, starting from just downstream of the highlight up to the propeller face. Based on the specified mass BC, the code computed a constant static pressure ratio of p_{loc}/P_0 = 0.83 over the propeller face plane. Comparing this calculated value of p_{loc}/P_0 with the cowl experimental static pressure ratio distribution in figure 6, shows that the experimental value is higher and varies circumferentially. This indicates the reason that the computational results, which evolved from using the mass BC at the propeller face, differ significantly from the test data on the leeward side. In figure 12(a) on the windward side (ϕ = 0°), the PARC3D calculation with the H-grid predicted a spike in static pressure at the highlight which appears unrealistic when compared with the test data. By using the HC-grid the PARC3D predicted a trend of static pressure which closely follows the test data. On the leeward side (fig. 12(b)), the predicted static pressure ratio distributions compare favorably with the test data and the difference in the grid format did not have any significant impact on the solutions.

Comparisons of total pressure distributions between experiment and PARC3D computation are shown in figure 13. The test data were obtained using two boundary layer rakes located axially at 0.17 D_{prop} upstream of the propeller face and at ϕ = 20° and ϕ = 160°, respectively. For this comparison only results obtained from the PARC3D computation using the fixed BC at the propeller face with the HC-grid are presented. In figure 13(a) at ϕ = 20° near the windward side, the predicted total pressure ratio distribution indicates that the flow boundary layer was thicker than the experimental flow boundary layer. Propeller pumping effects on the boundary layer were accounted for by utilizing the fixed BC (fig. 6). The difference in the boundary layers shown in figure 13(a) may be caused by the propeller induced effects (such as swirl) which were not accounted for in the PARC3D computation. In figure 13(b) at ϕ = 160° near the leeward side, the boundary layer, as indicated by the total pressure distribution, was thinner than that observed at ϕ = 20° near the windward side. The PARC3D prediction of total pressure distribution at this position provides a good comparison with the test data.

The results herein have shown that the Navier-Stokes based PARC code can be used to provide a reasonable prediction of the flow field for the ADP inlet. At an angle-of-attack of 0°, PARC2D with both the mass BC and the fixed BC using either the H- or the HC-grid for the propeller face provides a reasonable comparison with the experimental data. The comparison is shown in figures 8 and 9. PARC3D that must be used for a higher angle-of-attack operation provided a reasonable prediction of the inlet flow field when the fixed BC and the HC-grid were used. Comparison of analytical and experimental results for an angle-of-attack of 25° were shown in figures 12 and 13. The code prediction did deviate from the experimental data for the boundary layer profile near the windward side.

Summary

Viscous subsonic flow solutions were obtained for an experimental ADP inlet at α's of 0° and 25°. The flow solutions were computational results from the PARC code - PARC2D for axisymmetric and PARC3D for 3-D flow calculations. The objective of this analytical study was to validate the code for subsonic inlet applications. The inlet flow involved in this code validation study is non-separated flow. Two types of computational BC's were applied at the propeller face; namely, a mass BC and fixed BC. The latter was developed using data from an experimental study combined with calculated results from a panel code. With the mass BC, the computation was performed using only the HC-grid. With the fixed BC, it was performed using both the H-grid and the HC-grid.

The results herein have shown that the PARC code can be used to provide a reasonable prediction of the flow field within an inlet for an advanced ducted propeller. At an angle-of-attack of 0°, PARC2D with a mass BC or with a fixed BC for the propeller face provides a reasonable comparison with the experimental data. For this case, the difference in the grid format did not have any significant effect on the computational results. PARC3D that must be used for a higher angle-of-attack operation provides a reasonable prediction of the inlet flow field when the fixed BC and the HC-grid were used. The code prediction did deviate from the experimental data for the boundary layer near the windward side.

References

1. Boldman, D.R.; C. Iek; D.P. Hwang; R.J. Jeracki; M. Larkin; and G. Sorin: Evaluation of Panel Code with Experimental Results of Inlet Performance a 17-inch Ducted Prop/Fan Simulator Operating at Mach 0.2, AIAA 91-3354.

2. Lieblein, S.; and Stockman, N.O.: Compressibility Correction for Internal Flow Solution, Journal of Aircraft, Vol.9, April 1972, pp 312-313.

3. Pulliam, T.H.; and Steger, J.L.: Implicit Finite-Difference Simulations of Three-Dimensional Compressible Flow, AIAA Journal, Vol. 18, February 1980, pp. 159-167.

4. Pulliam, T.H.: Euler and Thin Layer Navier-Stokes Codes: ARC2D, ARC3D, Notes for Computational Fluid Dynamics User's Workshop, The University of Tennessee Space Institute, Tullahoma, Tennessee, March 12-16, 1984.

5. Jameson, A.; Schmidt, W.; and Turkel, E.: Numerical Solutions of the Euler Equations by Finite Volume Method Using Runge-Kutta Time Stepping Schemes, AIAA 81-1259.

6. Cooper, G.K.; Jordan, J.L.; and Phases, W.J.: Analysis Tool for Application to Ground Testing of Highly Underexpanded Nozzles, AIAA 87-2015.

7. Hess, J.L.; Mack, D.P.; and Stockman, N.O.: An Efficient User-Oriented Method for Calculating Compressible Flow in and About Three-Dimensional Inlets - Panel Method, NASA CR-159578, April 1979.

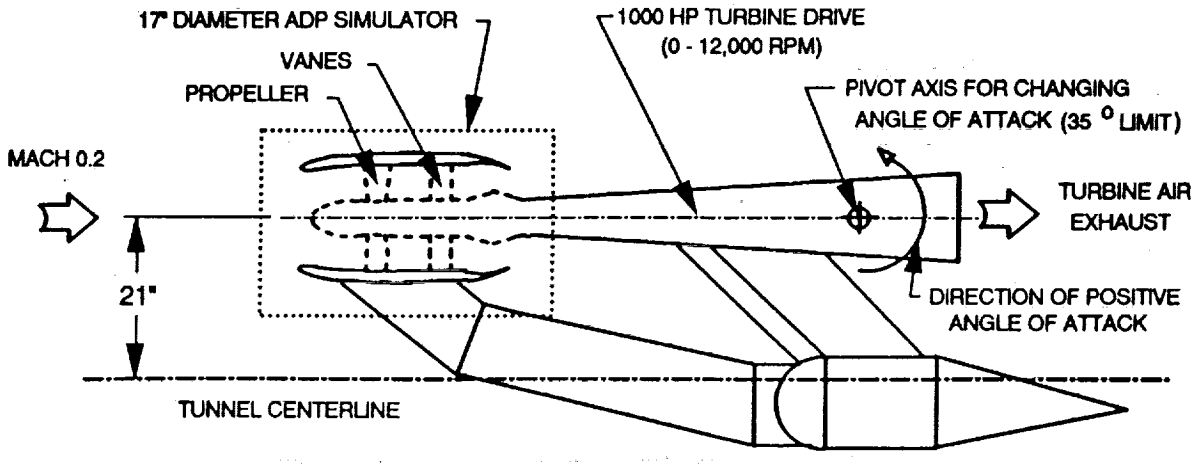

Fig. 1 Top view of installation of 17-inch ADP simulator in the 9 x 15 ft Low Speed Wind Tunnel.

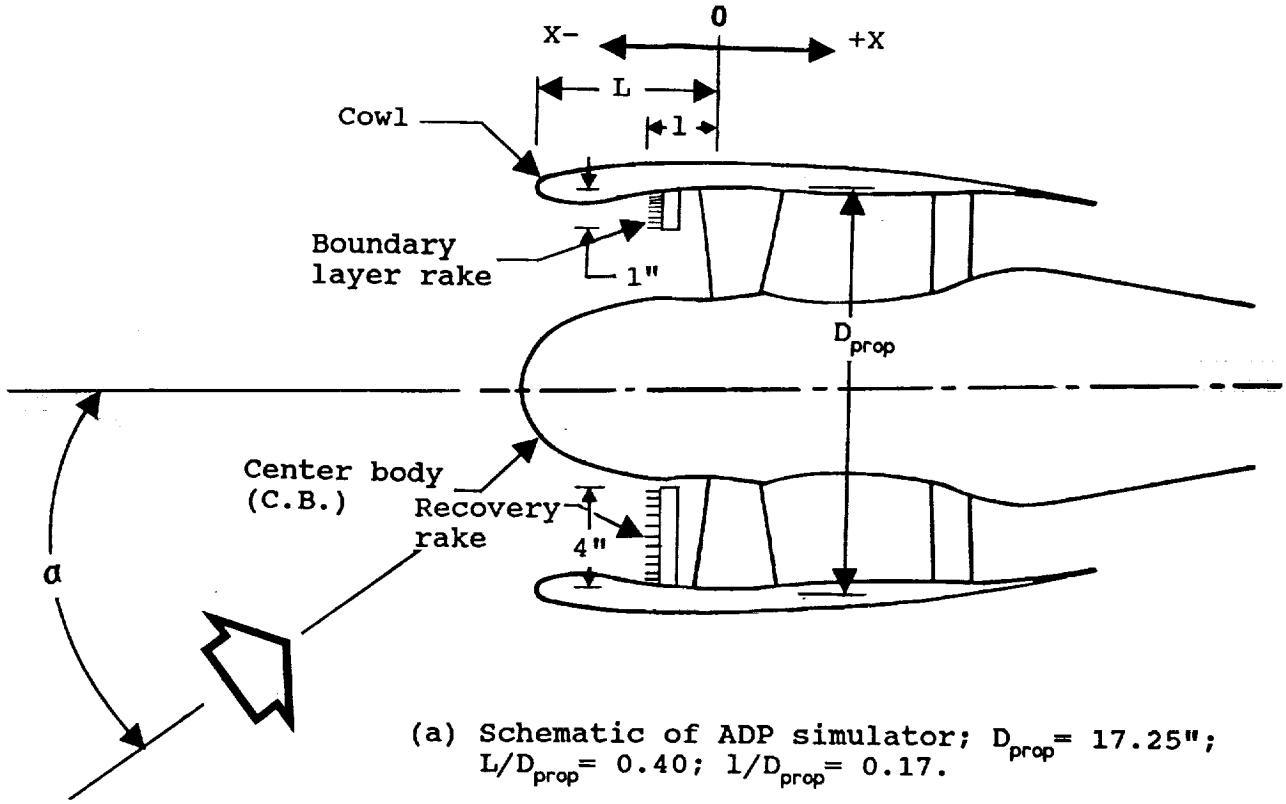

(a) Schematic of ADP simulator; D_{prop}= 17.25"; L/D_{prop}= 0.40; l/D_{prop}= 0.17.

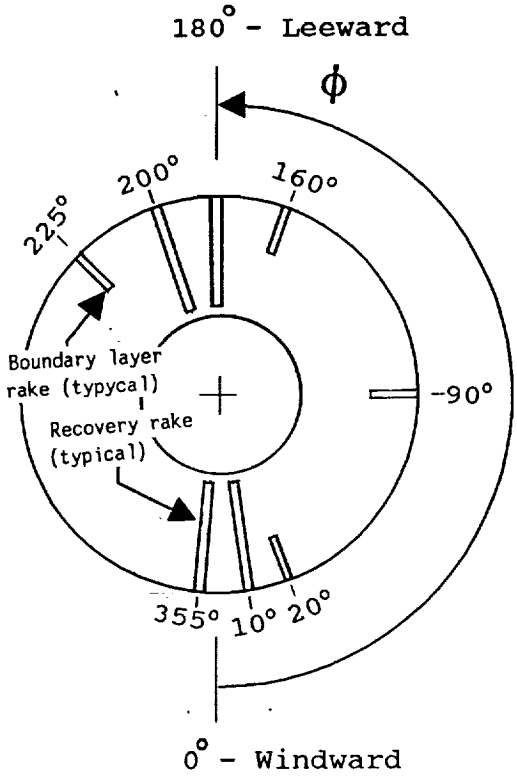

(b) Boundary layer rake arrangement; looking downstream.

Fig. 2 ADP simulator with boundary layer and recovery rakes arrangement.

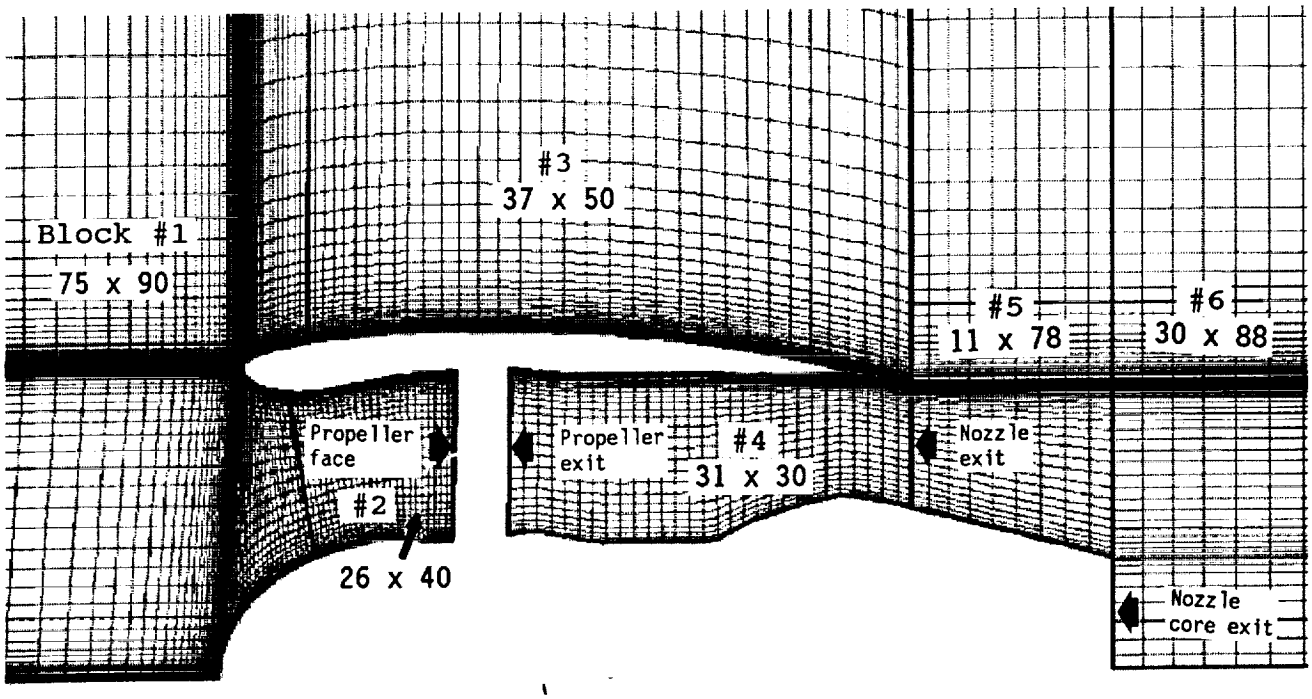

2-D H-grid

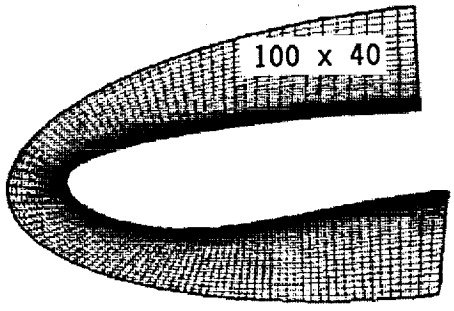

Cowl C-grid

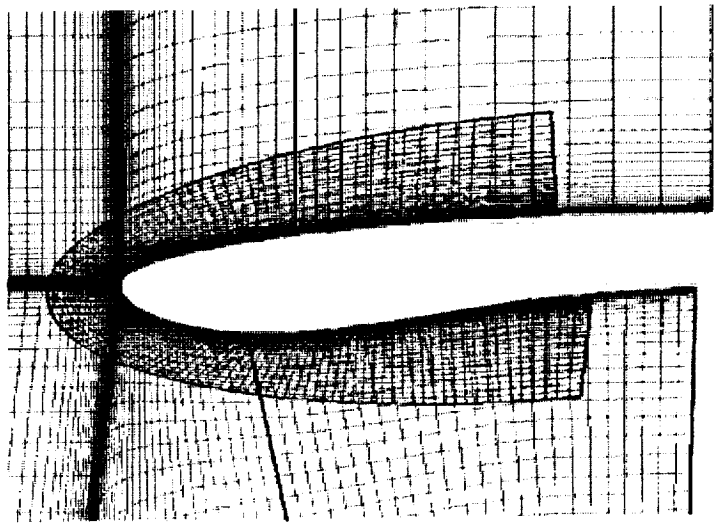

H-grid with embedded C-grid

Fig. 3 Computational grid for PARC2D axisymmetric (α = 0°) flow calculation.

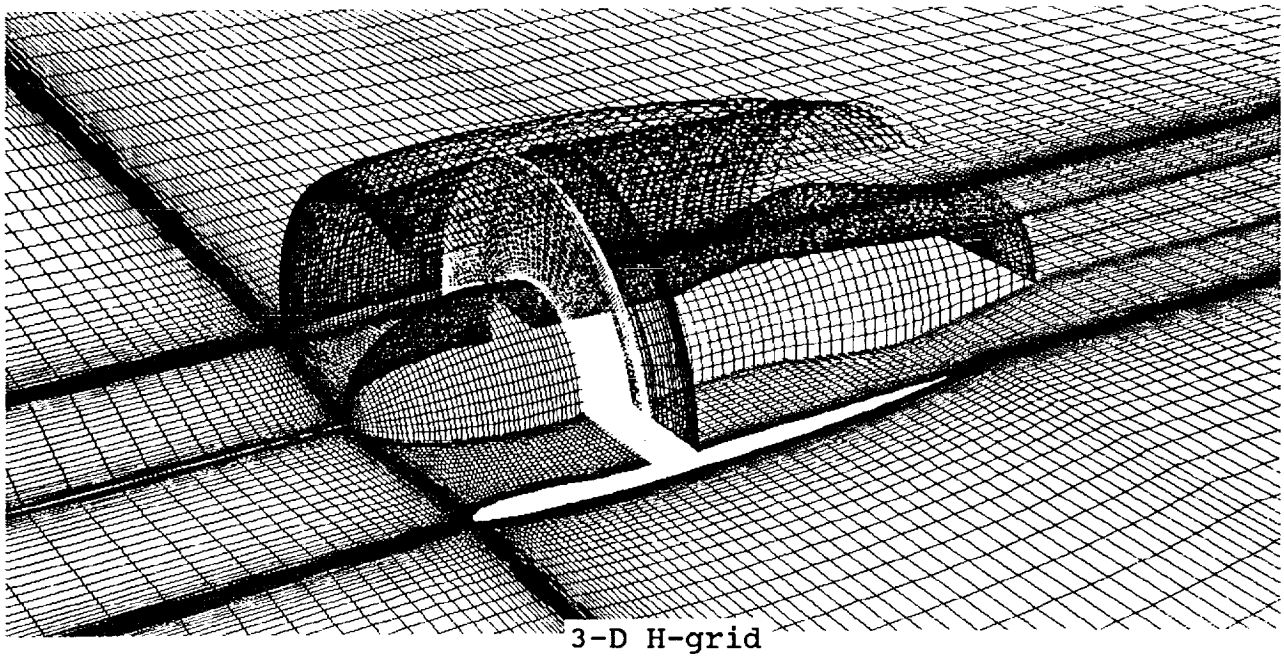

3-D H-grid

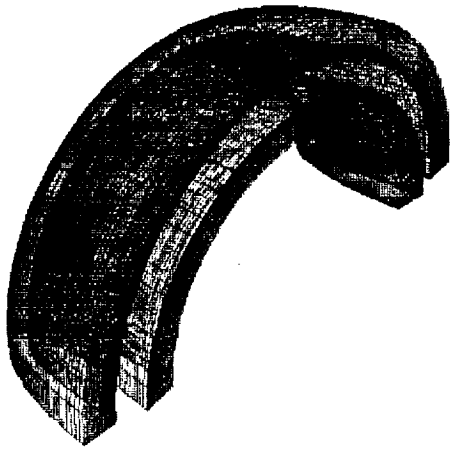

Cowl C-grid

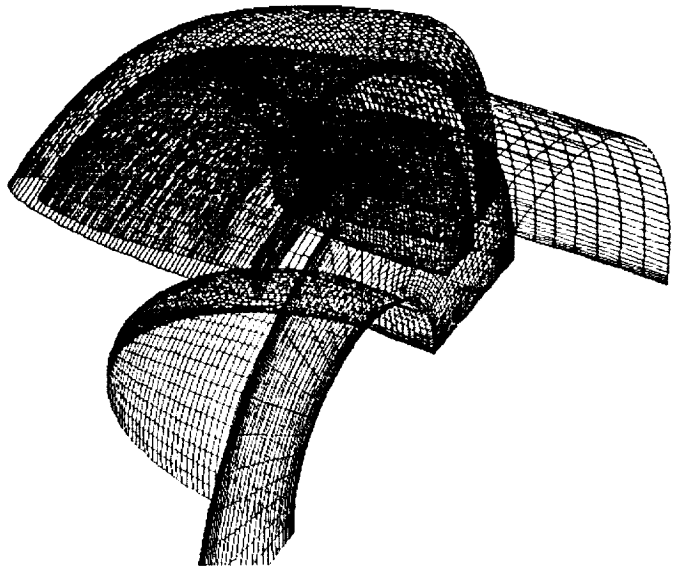

H-grid with embedded C-grid

Fig. 4 Computational grid for PARC3D (α = 25°) flow calculation.

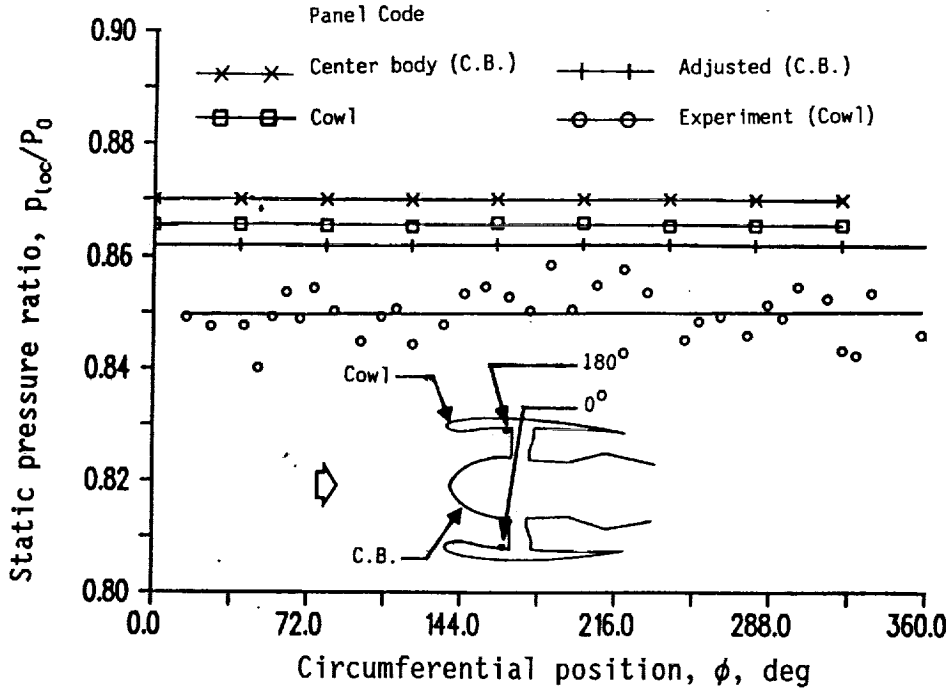

Fig. 5 Circumferential static pressure distributions obtained from the experiment and the panel code for M_0= 0.2, α = 0°, and W_c= 46.4 lb/sec.

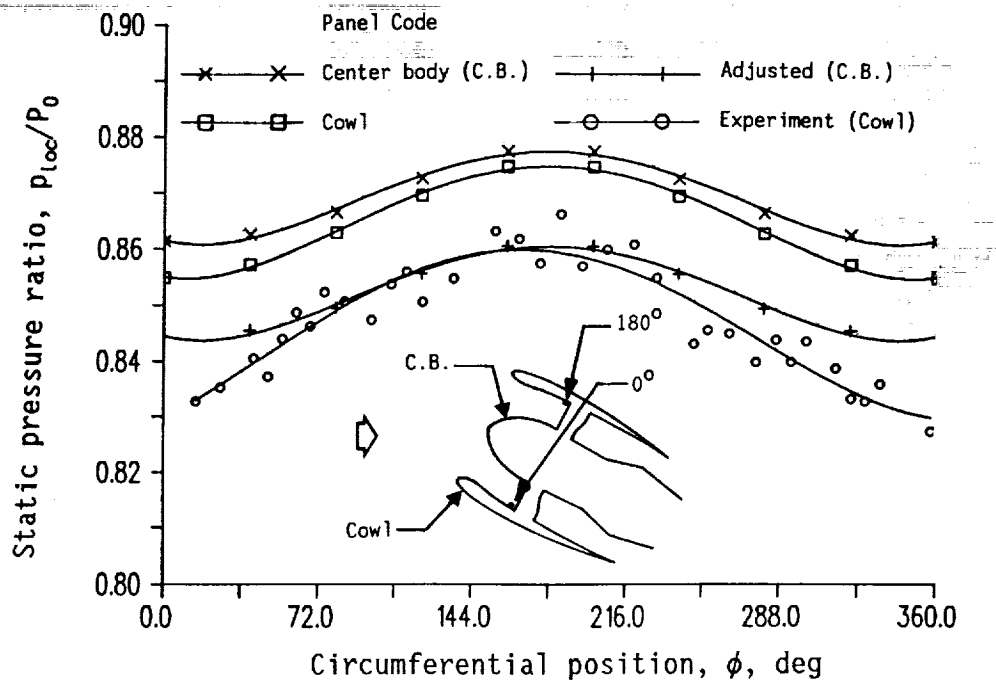

Fig. 6 Circumferential static pressure distributions obtained from the experiment and the panel code for M_0= 0.2, α = 25°, and W_c= 46.6 lb/sec.

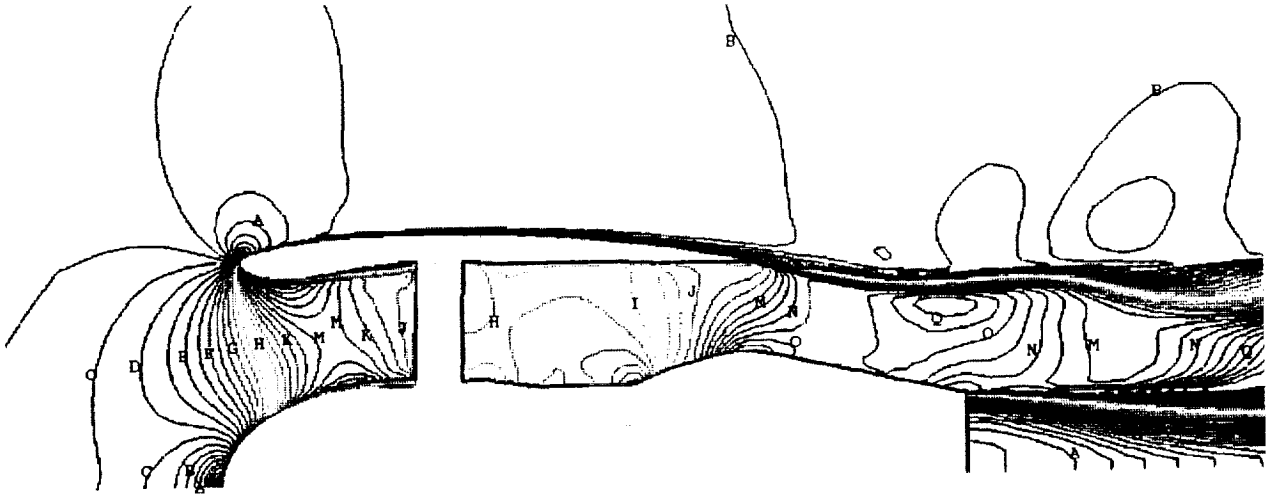

(a) Mach number contours over the computational domain.

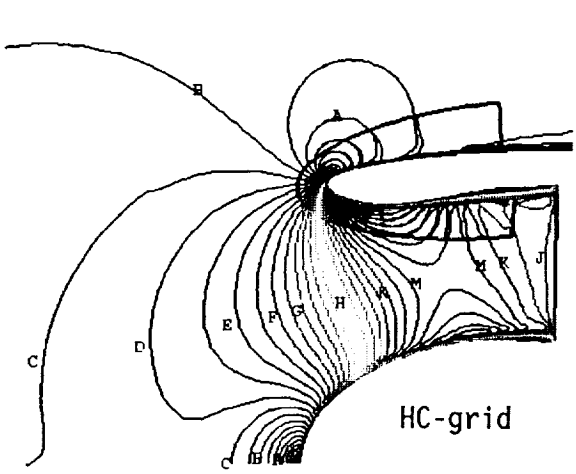

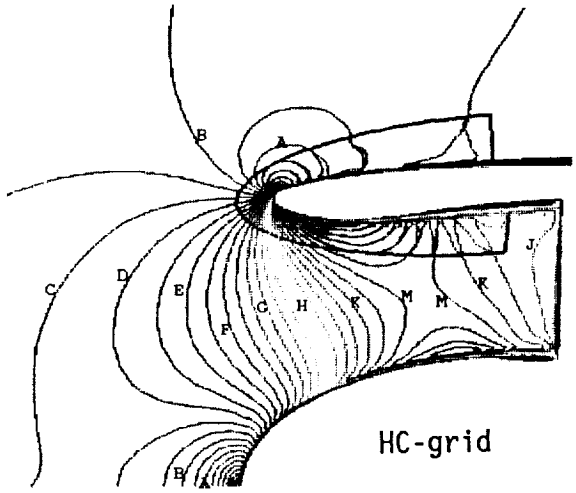

(b) Mach number contours using mass BC at the propeller face.

Mach number

A	0.16
B	0.20
C	0.22
D	0.24
E	0.28
F	0.34
G	0.38
H	0.44
I	0.46
J	0.48
K	0.50
L	0.52
M	0.54
N	0.56
O	0.60
P	0.62
Q	0.64

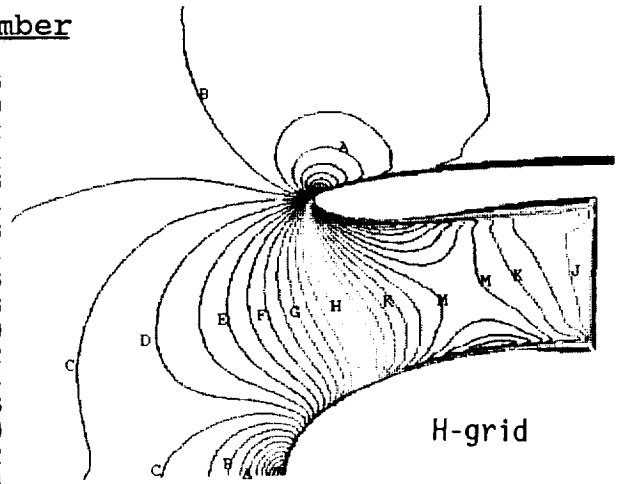

(c) Mach number contours using fixed BC at the propeller face.

Fig. 7 Mach number contours from PARC2D axisymmetric flow computation of the ADP inlet at $\alpha = 0^{\circ}$.

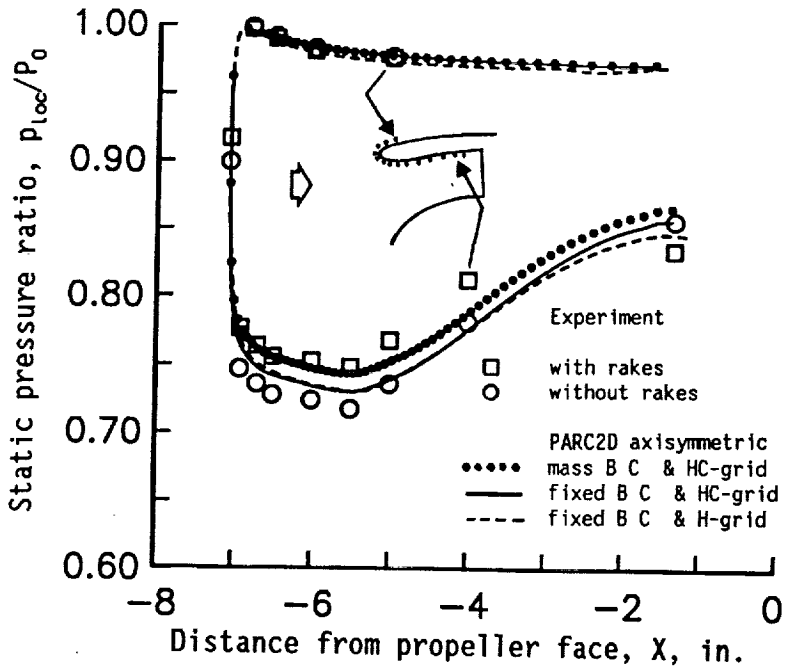

Fig. 8 Comparison of inlet cowl static pressure ratio distributions between experiment and PARC2D analysis for M_0= 0.2, α = 0°, and W_c= 46.4 lb/sec.

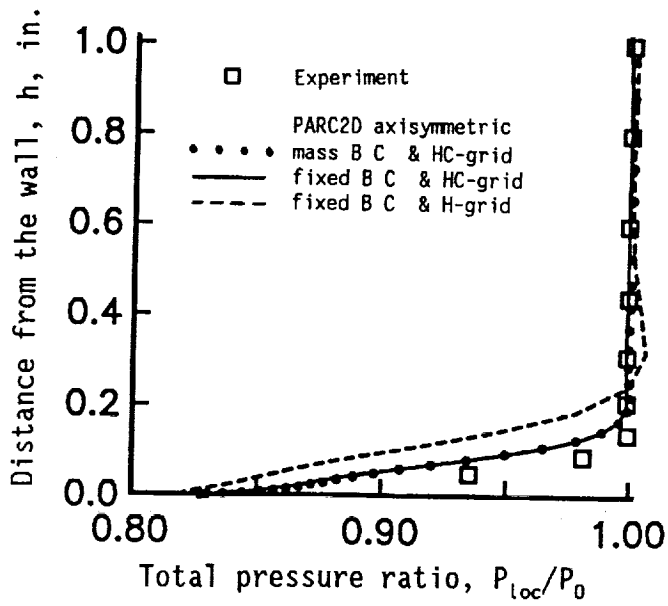

Fig. 9 Comparison of inlet boundary layer total pressure ratio distributions between experiment and PARC2D analysis for M_0= 0.2, α = 0°, and W_c= 46.4 lb/sec.

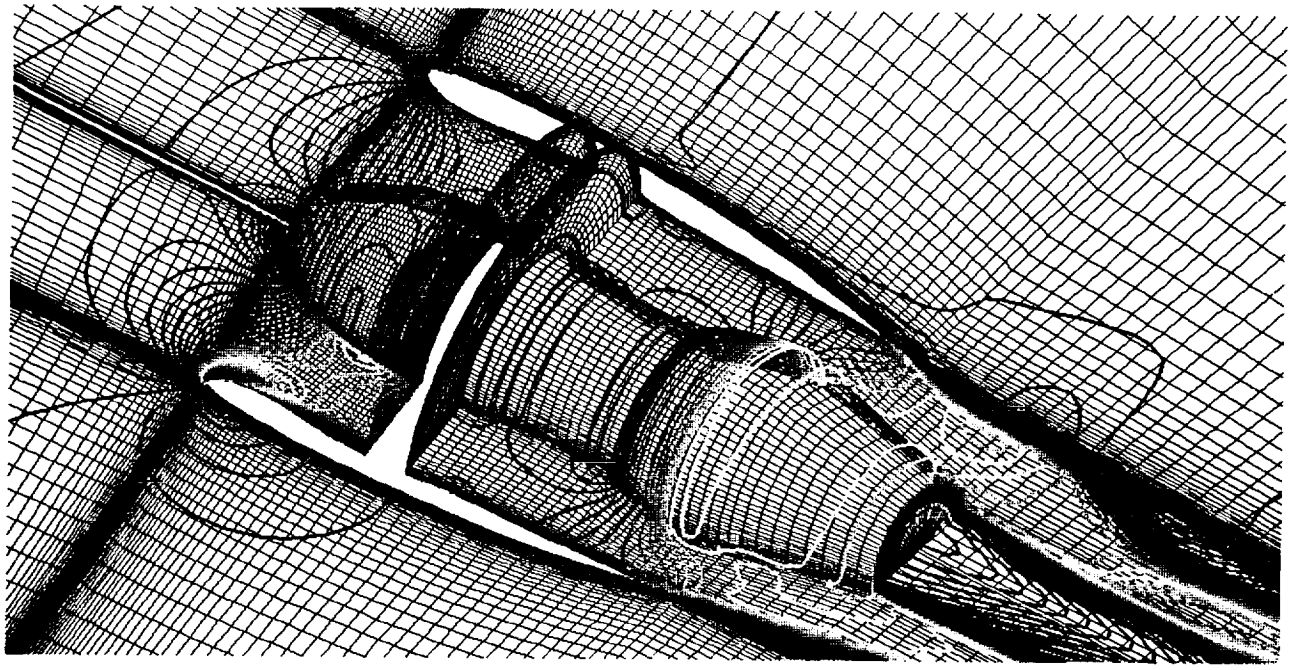

(a) Mach number contours over the computational domain.

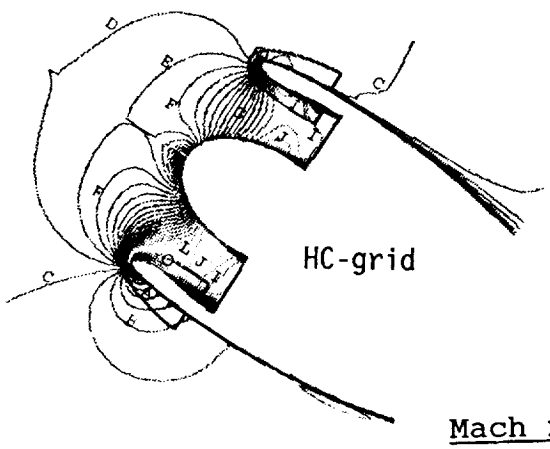

(b) Mach number contours using mass BC at the propeller face.

Mach number

A	0.07
B	0.12
C	0.19
D	0.22
E	0.24
F	0.29
G	0.36
H	0.43
I	0.48
J	0.53
K	0.56
L	0.58
M	0.62
N	0.67
O	0.70

Fig. 10 Mach number contours from PARC3D flow computation of the ADP inlet at α = 25°.

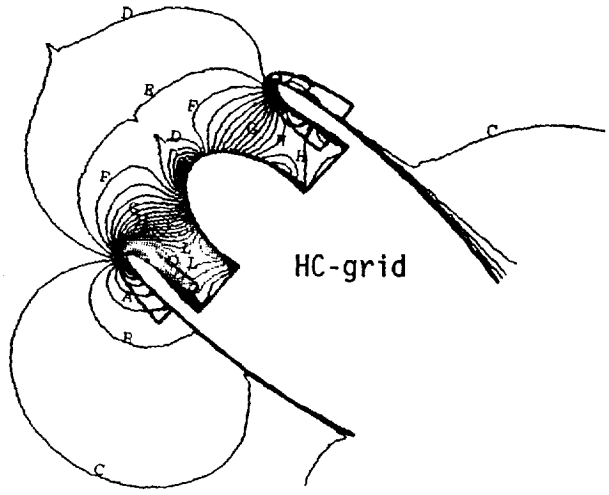

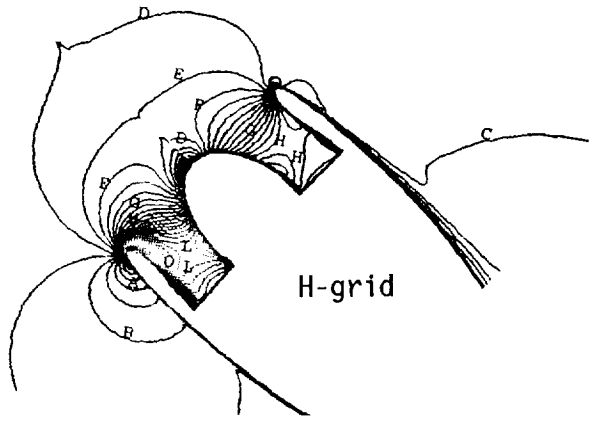

(c) Mach number contours using fixed BC at the propeller face.

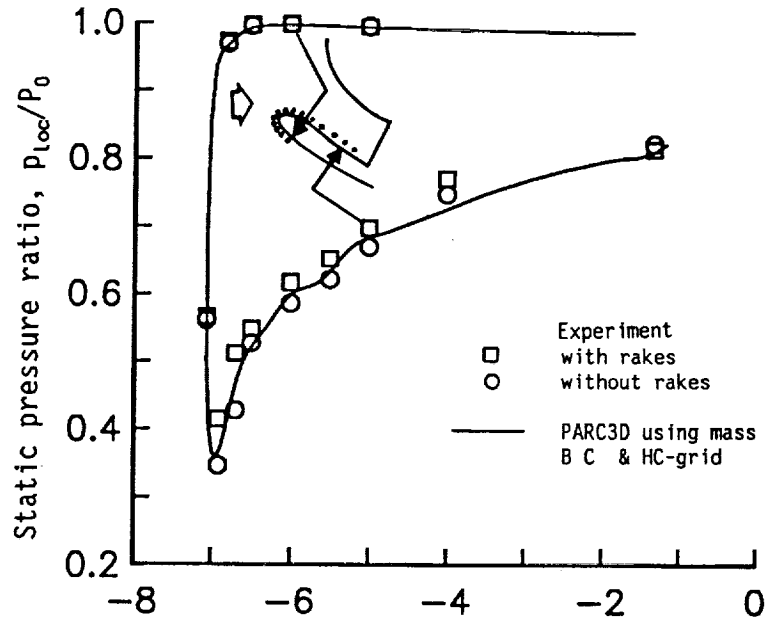

(a) Windward side (ϕ = 0°)

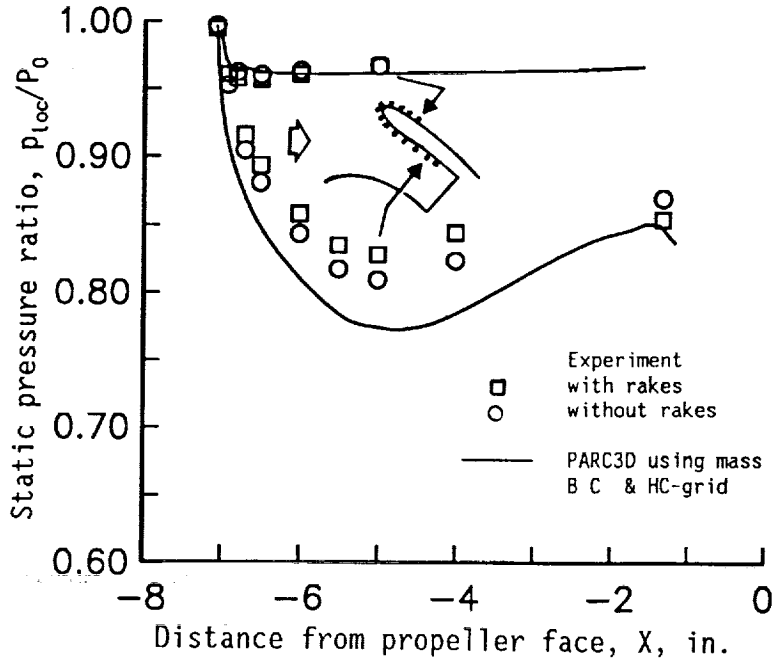

(b) Leeward side, ϕ = 180°

Fig. 11 Comparison of inlet cowl static pressure ratio distributions between experiment and PARC3D analysis using mass B C at the propeller face for M_0= 0.2, α = 25°, and W_c= 46.6 lb/sec.

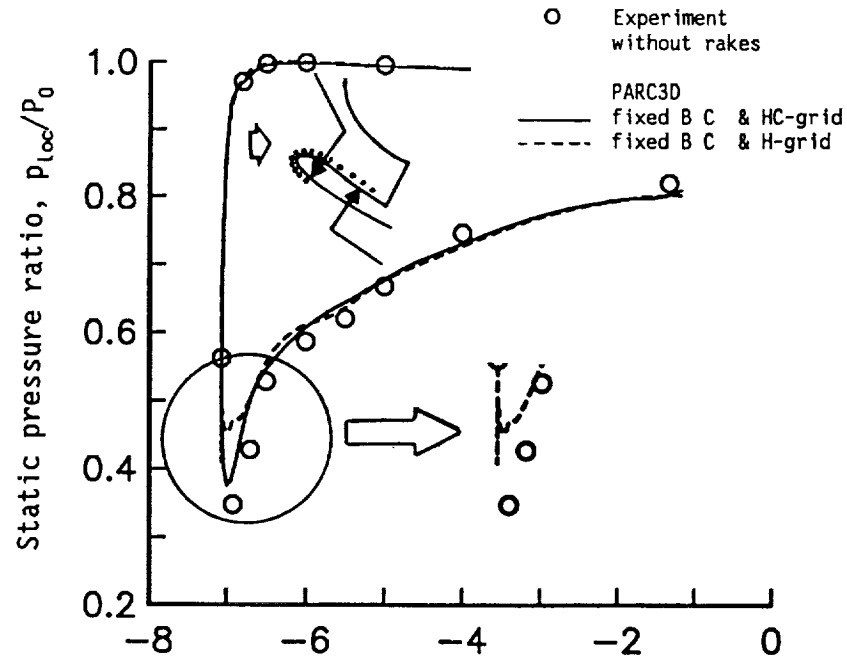

(a) Windward side (ϕ = 0°)

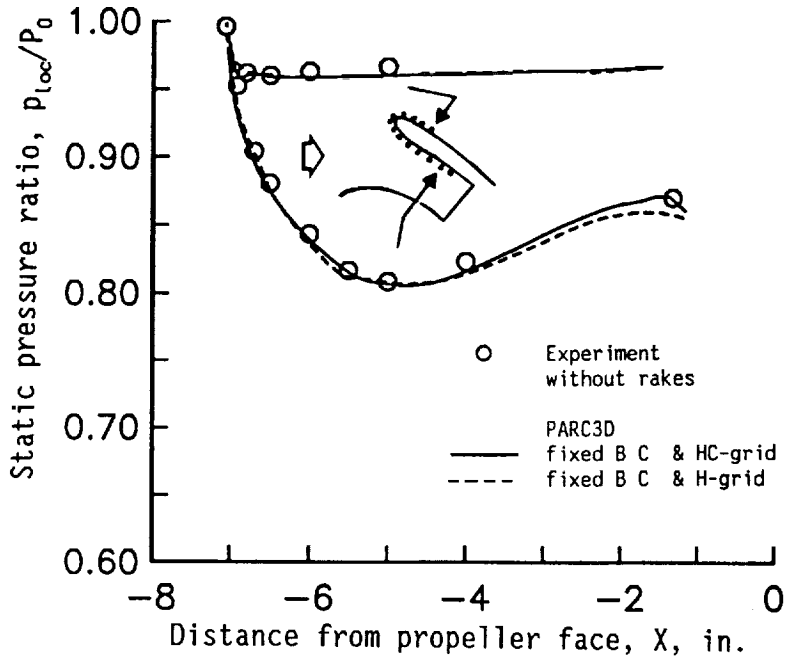

(b) Leeward side, ϕ = 180°

Fig. 12 Comparison of inlet cowl static pressure ratio distributions between experiment and PARC3D analysis using fixed B C at the propeller face for M_0= 0.2, α = 25°, and W_c= 46.6 lb/sec.

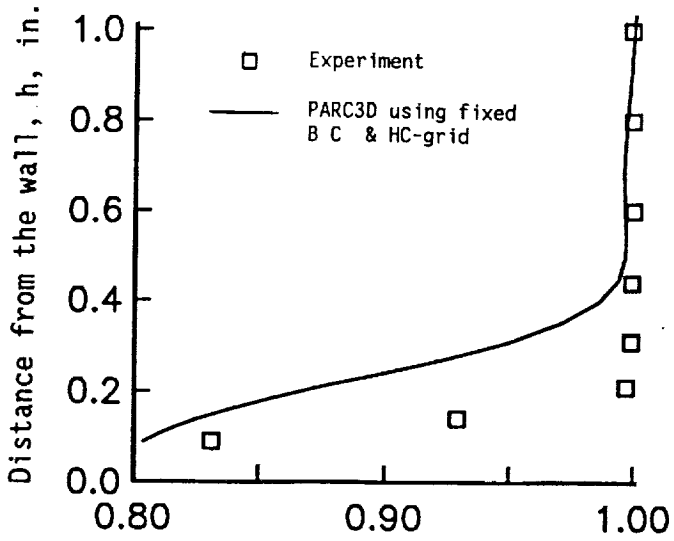

(a) Boundary layer rake near the windward side, ϕ = 20°.

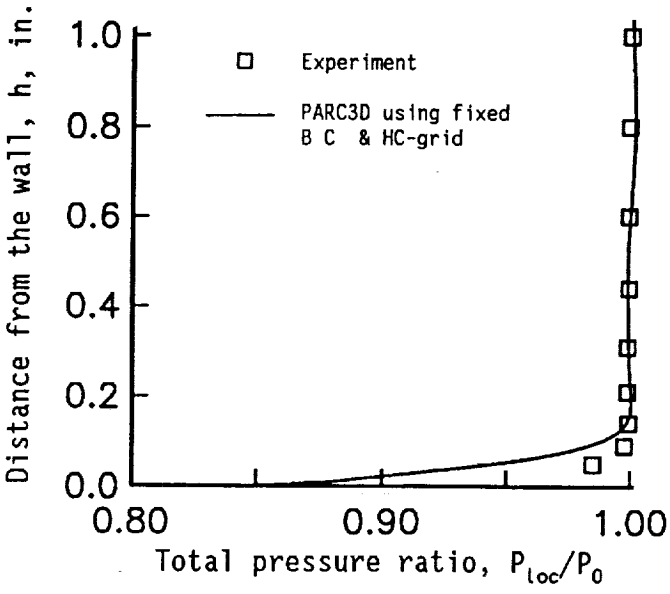

(b) Boundary layer rake near the leeward side, ϕ = 160°.

Fig. 13 Comparison of inlet boundary layer total pressure ratio distributions between experiment and PARC3D analysis using fixed B C at the propeller face for M_0= 0.2, α = 25°, and W_c= 46.6 lb/sec.

REPORT DOCUMENTATION PAGE

Form Approved
OMB No. 0704-0188

1. AGENCY USE ONLY (*Leave blank*)	2. REPORT DATE	3. REPORT TYPE AND DATES COVERED
	1992	Technical Memorandum

4. TITLE AND SUBTITLE

Analysis of an Advanced Ducted Propeller Subsonic Inlet

5. FUNDING NUMBERS

WU-535-03-10

6. AUTHOR(S)

Chanthy Iek, Donald R. Boldman, and Mounir Ibrahim

7. PERFORMING ORGANIZATION NAME(S) AND ADDRESS(ES)

National Aeronautics and Space Administration
Lewis Research Center
Cleveland, Ohio 44135-3191

8. PERFORMING ORGANIZATION REPORT NUMBER

E-6784

9. SPONSORING/MONITORING AGENCY NAMES(S) AND ADDRESS(ES)

National Aeronautics and Space Administration
Washington, D.C. 20546-0001

10. SPONSORING/MONITORING AGENCY REPORT NUMBER

NASA TM-105393
AIAA-92-0274

11. SUPPLEMENTARY NOTES

Prepared for the 30th Aerospace Sciences Meeting and Exhibit sponsored by the American Institute of Aeronautics and Astronautics, Reno, Nevada, January 6–9, 1992. Chanthy Iek and Donald R. Boldman, NASA Lewis Research Center; Mounir Ibrahim, Cleveland State University, Cleveland, Ohio 44115. Responsible person, Chanthy Iek, (216) 433-3897.

12a. DISTRIBUTION/AVAILABILITY STATEMENT

Unclassified - Unlimited
Subject Category 02

12b. DISTRIBUTION CODE

13. ABSTRACT (*Maximum 200 words*)

A time marching Navier-Stokes code called PARC (PARC2D for 2-D/axisymmetric and PARC3D for 3-D flow simulations) was validated for an advanced ducted propeller (ADP) subsonic inlet. The code validation for an advanced ducted propeller (ADP) subsonic inlet. The code validation was implemented for a non-separated flow condition associated with the inlet operating at angles-of-attack of 0° and 25°. The inlet test data were obtained in the 9 x 15 ft Low Speed Wind Tunnel at NASA Lewis Research Center as part of a cooperative study with Pratt and Whitney. The experimental study focused on the ADP inlet performance for take-off and approach conditions. The inlet was tested at a free stream Mach number of 0.2, at angles-of-attack between 0° and 35°, and at a maximum propeller speed of 12,000 RPM which induced a corrected air flow rate of about 46 lb/sec based on standard day conditions. The computational grid and flow boundary conditions (BC) were based on the actual inlet geometry and the tunnel flow conditions. At the propeller face, two types of BC's were applied; namely a mass flow BC and a fixed flow properties BC. The fixed flow properties BC was based on a combination of data obtained from the experiment and calculations using a potential flow code. Comparison of the computational results with the test data indicates that the PARC code with the propeller face fixed flow properties BC provided a better prediction of the inlet surface static pressures than the prediction when the mass flow BC was used. For an angle-of-attack of 0°, the PARC2D code with the propeller face mass flow BC provided a good prediction of inlet static pressures except in the region of high pressure gradient. With the propeller face fixed flow properties BC, the PARC2D code provided a good prediction of the inlet static pressures. For an angle-of-attack of 25° with the mass flow BC, the PARC3D code predicted static pressures which deviated significantly form the test data; however, with the fixed flow properties BC, a good comparison with the test data was obtained.

14. SUBJECT TERMS

Navier-Stokes equations; Computational fluid dynamics; Air intakes; Engine inlets; Boundary layer analysis; Shrouded propellers

15. NUMBER OF PAGES

18

16. PRICE CODE

A03

17. SECURITY CLASSIFICATION OF REPORT	18. SECURITY CLASSIFICATION OF THIS PAGE	19. SECURITY CLASSIFICATION OF ABSTRACT	20. LIMITATION OF ABSTRACT
Unclassified	Unclassified	Unclassified